Hindawi
Advances in Civil Engineering
Volume 2019, Article ID 4572196, 16 pages
https://doi.org/10.1155/2019/4572196

Research Article

Numerical and Experimental Investigation of the Mechanical Behavior of Cable-Supported Barrel Vault Structures with Varying Temperature

Guojun Sun,[1,2] **Mingze Wu**,[3] **Zhihua Chen**,[4] **and Suduo Xue**[2,5]

[1]*Lecturer, Collage of Architecture and Civil Engineering, Beijing University of Technology, Beijing, China*
[2]*The Key Laboratory of Urban Security and Disaster Engineering, MOE, Beijing University of Technology, Beijing 100124, China*
[3]*M. A. Student, Collage of Architecture and Civil Engineering, Beijing University of Technology, Beijing, China*
[4]*Professor, Collage of Architecture and Civil Engineering, Tianjin University, Tianjin, China*
[5]*Professor, Collage of Architecture and Civil Engineering, Beijing University of Technology, Beijing, China*

Correspondence should be addressed to Guojun Sun; sunny2369@163.com

Received 25 December 2018; Revised 5 May 2019; Accepted 20 May 2019; Published 10 June 2019

Academic Editor: Giosuè Boscato

The cable-supported barrel vault (CSBV) structure system is a new type of hybrid spatial steel structure based on a beam string structure (or truss string structure), suspendomes, and cylindrical lattice shells. Steel cables (e.g., steel wire rope cables, steel strand cables, semiparallel steel tendons, and steel rods) are key components of CSBV structures. However, they have different elastic moduli and thermal expansion coefficients. In this study, the roof of a textile workshop (the first CSBV structure in China) was analyzed with four types of cables under the effect of varying temperature. Under half-span loading and full-span loading, the structural internal force and displacement at varying temperatures were obtained from finite element models employing four different types of steel cables. The internal force, displacement, and horizontal arch thrust changed linearly with increasing temperature. Moreover, the dynamic characteristics of CSBV with varying temperature were analyzed. The frequency of the CSBV changed linearly with increasing temperature. Based on the dynamic characteristics of CSBV with varying temperature, a seismic response time-history analysis was performed. The variation in the maximum responses of the internal force, displacement, and horizontal arch thrust was obtained. In each case, the mechanical behavior of the CSBV with semiparallel steel tendon cables was strongly affected by the temperature. Therefore, semiparallel steel tendons are not recommended as components of CSBV in cases where large temperature changes can be expected. Thereafter, a scale model of a CSBV was designed and used for experiments and corresponding finite element analyses under varying temperature. Experimental results show that the finite element method is effective for analyzing the mechanical behavior of CSBV under varying temperature.

1. Introduction

The static and dynamic performance of cable-supported barrel vault (CSBV) structures has been investigated using numerical and experimental methods, and superior static and dynamic performance compared to barrel vault structures has been demonstrated [2, 3]. In addition, a series of theoretical analyses and experimental studies have been carried out on the string structure, including form-finding analyses [4–6], structural optimization [7, 8], static behavior analyses [9–11], dynamic characteristics and seismic response analyses [12], prestress design methods [13], sensitivity analyses [14], and stability studies [15–18]. As a critical load-carrying member of CSBV structures, the cables are of primary importance for guaranteeing the safety of the entire structure. Steel cables are spun helically from different types of steel wires in several layers, and as a result, the thermal expansion properties of steel cables differ from those of steel. Therefore, different cable twist qualities can also affect the value of the thermal expansion coefficient [19, 20]. The

thermal expansion coefficient of a cable member is larger than that for a common steel member. Therefore, a loss of prestress occurs in cables at higher temperatures, while an increase in the cable prestress occurs at lower temperatures. In other words, the effect of temperature on the mechanical behavior of CSBV structures is more complicated than on common steel structures. Therefore, the effect of temperature on the mechanical behavior of CSBV structures still requires further research.

In this study, four CSBV structure models were designed with different cable materials: steel rods, steel wire cables, steel stand cables, and semiparallel steel tendons. The mechanical behavior of the CSBV structures under the effect of varying temperature was investigated using numerical analyses. In addition, an experimental study of the CSBV model structure with steel strand cables was carried out. The numerical and experimental results were then compared. Finally, some conclusions have been drawn for use in practical engineering applications.

2. Temperature Response Analysis

2.1. Example Analysis and Numerical Model. The project analyzed in this study is the first CSBV structure in China: the roof of a textile workshop. The roof is 410 m long and is divided into four parts. One of these four parts with a length of 116.2 m is analyzed; its span is 50 m. According to the demand of the architecture, the rise of this CSBV structure is 4.3 m and the sag is 0.7 m. The grid pattern of the upper single-layer lattice shell is a three-way lattice grid with a grid size of approximately 4.5 m. For the rod section, three different sections are selected: Φ305 mm × 10 mm, Φ229 mm × 8 mm, and Φ187 mm × 8 mm. The sections of the struts are all Φ253 mm × 10 mm. All cables have sections of Φ7 mm × 73 mm, and the ultimate tensile strength of the cables is 1860 MPa. The roof dead load is 0.80 kN/m^2, and the roof live load is 0.50 kN/m^2. The building perspective, plane graph, and elevation drawing are shown in Figures 1(a), 1(b), and 1(c), respectively.

The prestress design principle of the CSBV, in which the peripheral restriction is usually a spatial pin, is that the horizontal arch thrust is zero. First, no prestress is applied, i.e.,the prestress of each cable is zero. Thus, subjected to the dead weight of the structure itself, the horizontal arch thrusts can be calculated. Then, the structure is reanalyzed, and the obtained horizontal arch thrusts are applied to each cable. By performing the calculation again, a new horizontal arch thrust is obtained, changing the calculated prestress, which can then be used to recalculate the horizontal arch thrust again. This iterative process is repeated until the horizontal arch thrust is zero or close to zero, at which point the calculated prestress applied to the cables is defined as the target value. It should be noted that the geometric nonlinearity of the structure must be considered in the above calculation process. The whole process can be performed with general finite element analysis software such as ANSYS. In the ANSYS APDL finite element software package, the beam188 element was adopted to simulate the steel members in the upper vault structure, while the struts and cables were simulated with link8 and link10 elements, respectively.

In this study, four CSBV structure models were designed with different cable materials: steel rods, steel wire cables, steel stand cables, and semiparallel steel tendons. The elastic modulus and thermal expansion coefficient of the four steel cable types are listed in Table 1. The elastic modulus and thermal expansion coefficient of the upper beam and strut were assumed to be 2.06×10^5 MPa and 1.2×10^{-5}/°C, respectively. The mechanical behavior was obtained for the temperature range of −40°C to +40°C. The abbreviation SR indicates the CSBV structure with cable rods, SRC represents the CSBV with steel wire rope cables, SSC represents the CSBV with the steel strand cables, and SST represents the CSBV with semiparallel steel tendons.

2.2. Numerical Simulation of the CSBV with Full-Span Load Distribution. Considering the practical conditions, the CSBV structure is subject to a dead load and a live load in the vertical direction. The vertical load is calculated using a load condition of 1.2 × dead load + 1.4 × live load. Therefore, the numerical load on the whole roof is designed to be approximately $1.2 \times 0.8\ \text{kN/m}^2 + 1.4 \times 0.5\ \text{kN/m}^2 = 1.66\ \text{kN/m}^2$. The Surf 154 element is used to achieve full-span loading of the structure in this study. The temperature load is reduced by 40°C and increased by 40°C.

The vertical displacements of the node in the midframe and end-frame are shown in Figure 2 for Nodes 1–4. Figure 2 also shows the cable forces in the midframe and end-frame for Cables 1 and 2, the upper structural steel member (USSM) forces at the midframe and end-frame for USSM 1–4, the strut force in midframe and end-frame for Struts 1–4, and the horizontal arch thrust (HAT) in the midframe and end-frame for HAT 1 and 2.

Then, a nonlinear analysis of the CSBV structures was carried out. The results and influence of the temperature on the full-span load distribution were obtained. For example, in the full-span load distribution, the relationship between the vertical displacement of the nodes and the temperature is approximately linear.

In Figure 3, a positive sign represents an upward displacement and a negative sign represents a downward displacement. The displacements of the nodes increase with increasing temperature. The displacement trends for Node 2 and Node 4 are similar to those of Node 3, which is shown in Figure 3(b). Meanwhile, Figure 3(a) shows that the change in the displacement of the SST cables is slightly less than that of the other structures, but it can also be approximated as a linear variation.

The influence of the temperature on the cable force in the full-span load distribution is presented in Figure 4. Figure 4(a) shows the change in the cable force in the end-frame, and Figure 4(b) shows the change in the cable force in the midframe; the positive sign represents a tension force. The cable force decreases linearly with increasing temperature. The cable forces at the midframe are larger than those at the end-frame. Moreover, the SST cable force exhibits the

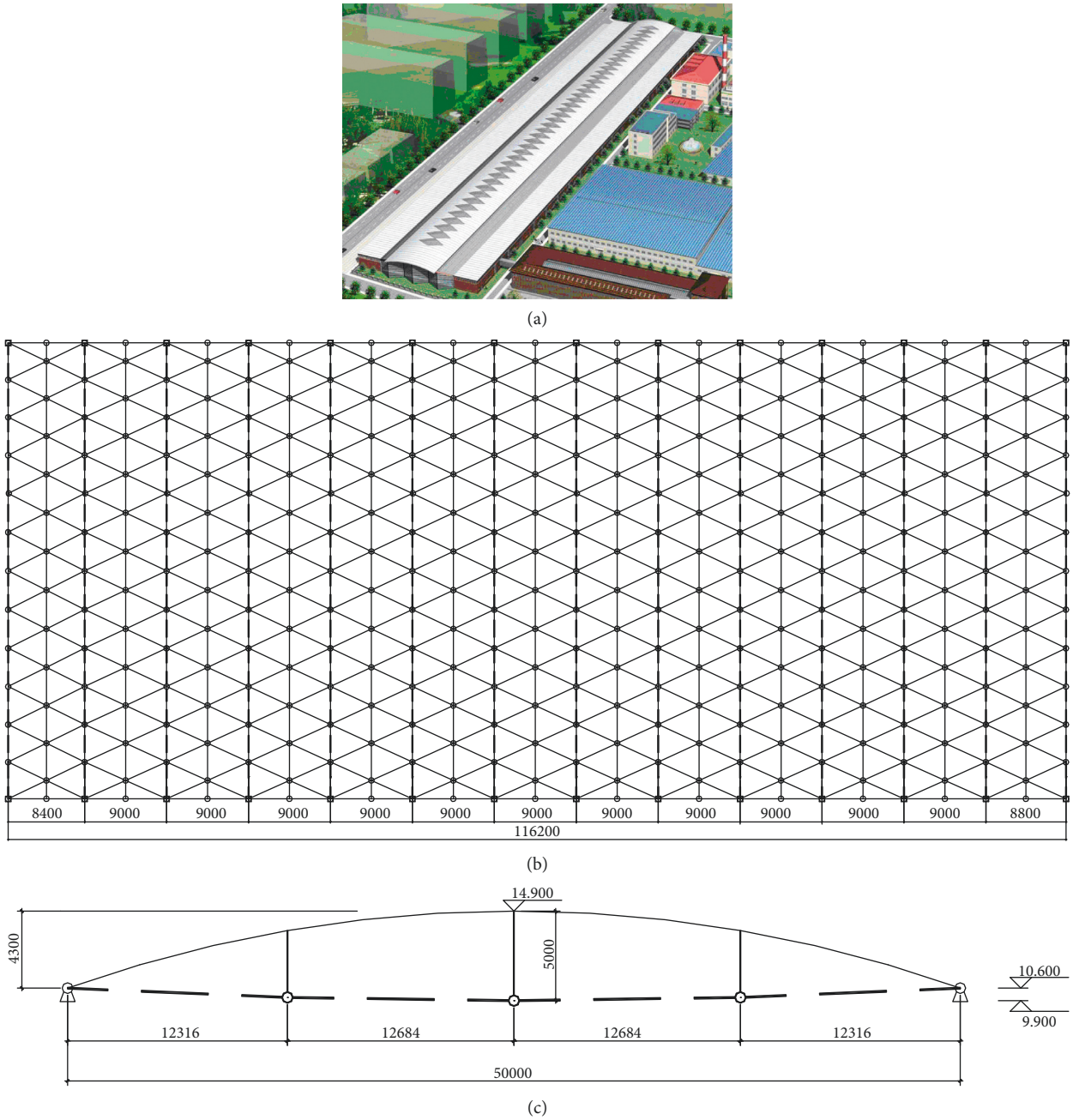

Figure 1: Elevation and plane graph of the CSBV structure. (a) Building perspective. (b) Plane graph of the CSBV (units: mm). (c) Elevation of the CSBV (units: mm).

Table 1: Modulus of elasticity and thermal expansion coefficient of the four types of cables.

Types	Steel rod	Steel wire rope cable	Steel strand cable	Semiparallel steel tendon
Elastic modulus ($\times 10^5$ MPa)	2.06	1.4	1.95	2.05
Thermal expansion coefficient ($\times 10^{-5}$/°C)	1.195	1.92	1.38	1.87

largest change with the temperature. Thus, the cable force of the CSBV with semiparallel steel tendons changes more than that of the CSBV with the other three types of cables owing to the large elastic modulus and thermal expansion coefficient of the SST cables.

Figure 5 shows the relationship between the strut force and the temperature under the full-span load; the negative sign represents a pressure force. The change in the strut force with temperature is approximately linear, and the strut forces decrease with increasing temperature. The strut

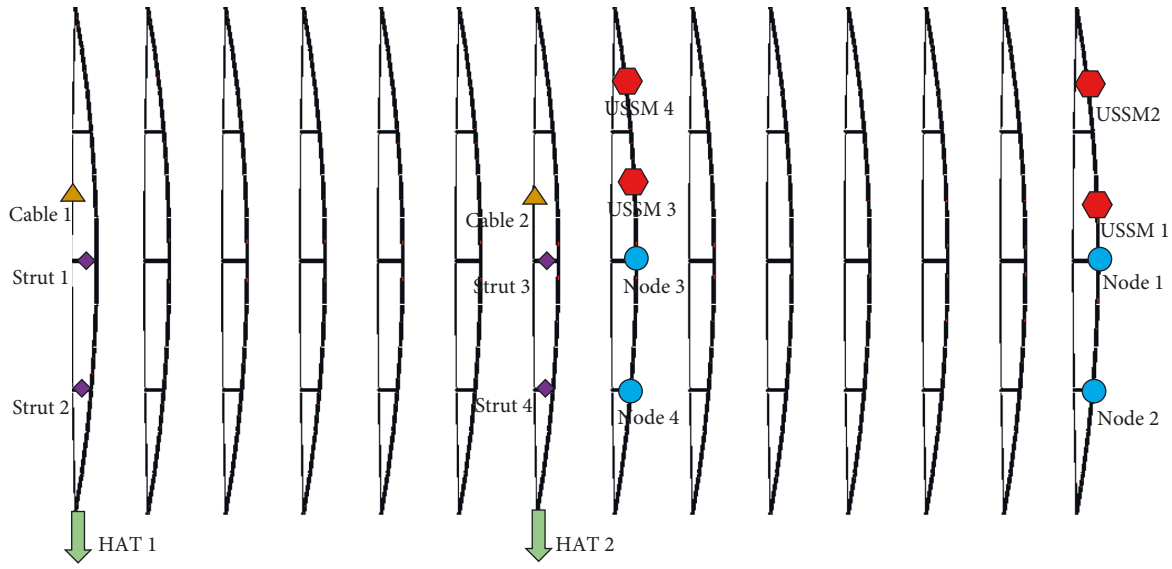

Figure 2: Targets of the numerical simulation analysis with a full-span load distribution.

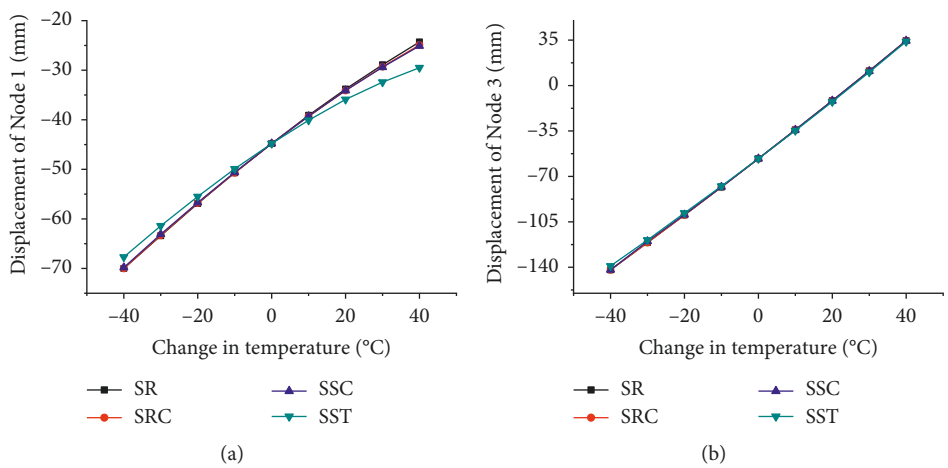

Figure 3: Relationship between the displacement and temperature in the full-span load distribution. Displacement of (a) Node 1 and (b) Node 3 with varying temperature.

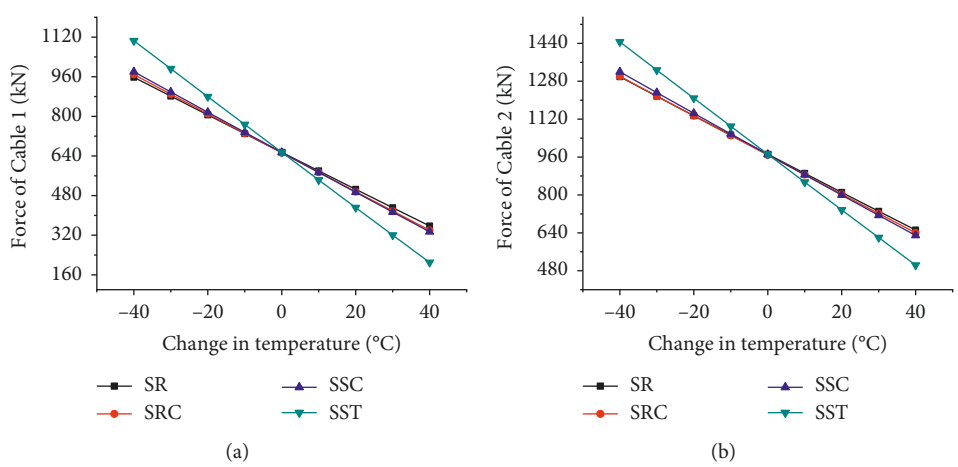

Figure 4: Relationship between the cable force and the temperature in the full-span load distribution. Change in the cable force of (a) Cable 1 and (b) Cable 2 with varying temperature.

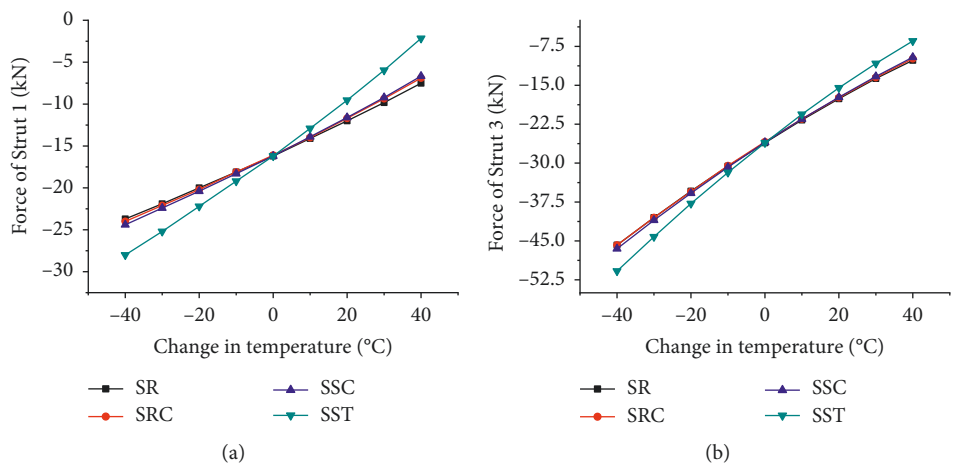

Figure 5: Relationship between the strut force and the temperature in the full-span load distribution. Change in the strut force of (a) Strut 1 and (b) Strut 3 with varying temperature.

pressure forces in Strut 1 and Strut 2 are lower than the strut pressure forces in Strut 3 and Strut 4. Moreover, the strut force of the CSBV with semiparallel steel tendon cables is more sensitive to the effect of temperature than the CSBV with the other cable types. This is similar to the change observed in the cable force. Therefore, the influence of temperature on the force of the vertical struts is related to the prestress of the cable. However, the influence on the force of the vertical struts is not completely in accordance with the prestress of the cable owing to the self-thermal stresses of the struts.

Figure 6 shows the influence of the temperature on the force of the USSM in the full-span load distribution; the negative sign indicates a pressure force. The relationship between the temperature and the USSM force is linear, except for in USSM 1. Moreover, the change in the force of USSM 1 under the effect of temperature is far less than its own force. Therefore, the force of USSM 1 can be considered to change linearly under the effect of temperature. The pressure force of the midframe USSM decreases with increasing temperature. In the end-frame, except for USSM 4, the USSM forces at the midspan and at the end-span decrease and increase, respectively, with increasing temperature. The force of USSM 4 in end-frame decreases under the effect of temperature. Moreover, the USSM force of the CSBV structure with semiparallel steel tendon cables is more sensitive to temperature changes. Therefore, the influence of temperature on the USSM force is related to the prestress of the cable. However, the influence of temperature on the force of the vertical struts is not completely in accordance with the prestress of the cable owing to the self-thermal stresses of the USSM.

Figure 7 shows the influence of the temperature on the horizontal arch thrust in the full-span load distribution; a negative sign represents an opposite horizontal arch thrust, i.e.,the horizontal arch produces tension. The horizontal arch thrust in every structure changes linearly with the temperature. Moreover, the horizontal arch thrust increases with increasing temperature. When the semiparallel steel tendon cable is selected, the change in the horizontal arch thrust is more pronounced under the effect of temperature. Note that the horizontal arch thrust could be negative at low temperatures. In other words, the horizontal arch thrusts could become tensile forces when the optimization goal of the cable prestress state is a zero horizontal arch thrust in the design process of the CSBV.

2.3. Numerical Simulation of the CSBV with Half-Span Load Distribution. Half-span loading was conducted using element surf 154, and the loading area is shown in Figure 8. The temperature change is ±40°C. Figure 8 shows the vertical displacements of the nodes in the midframe and end-frame for Nodes 1–6, the cable axial force in the midframe and end-frame for Cables 1–8, the USSM force in the midframe and end-frame for USSM 1–4, the strut force in the midframe and end-frame for Struts 1–6, and the HAT in the midframe and end-frame for HAT 1–4.

Figure 9 shows the influence of the temperature on the vertical displacement of nodes in the half-span load distribution; a positive sign represents an upward displacement, and a negative sign represents a downward displacement. Node 3 and Node 6 are located in the area with the load, and their displacement evolution is complex but small. Besides Node 3 and Node 6, the displacement changes of the other nodes are similar to that of Node 1, which is shown in Figure 9(a). The displacements in these cases all increase linearly with increasing temperature. Moreover, the displacement change of the CSBV with the semiparallel cables is different than that of the CSBV with the other three cables.

The influence of the temperature on the cable force in the half-span load distribution is presented in Figure 10. Figure 10(a) shows the change in the cable force at the end-frame, and Figure 10(b) shows the change in the cable force at the midframe; the positive sign represents a tension force. The cable forces at the midframe are larger than those at the end-frame. The change in the cable force with temperature is similar to that at full load. The cable force decreases linearly with increasing temperature. Moreover, the cable force of the SST cables exhibits greater changes with the temperature,

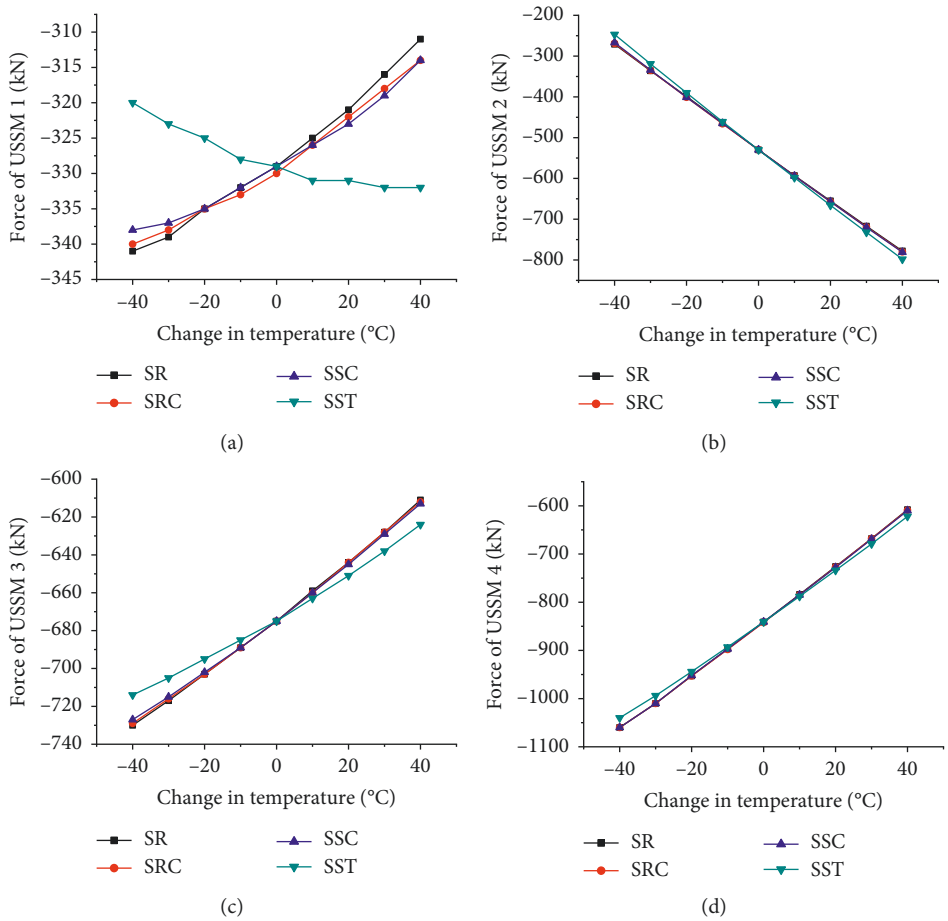

Figure 6: Relationship between the force at the upper structural steel members and the temperature in the full-span load distribution. Change in the force of (a) USSM 1, (b) USSM 2, (c) USSM 3, and (d) USSM 4 with varying temperature.

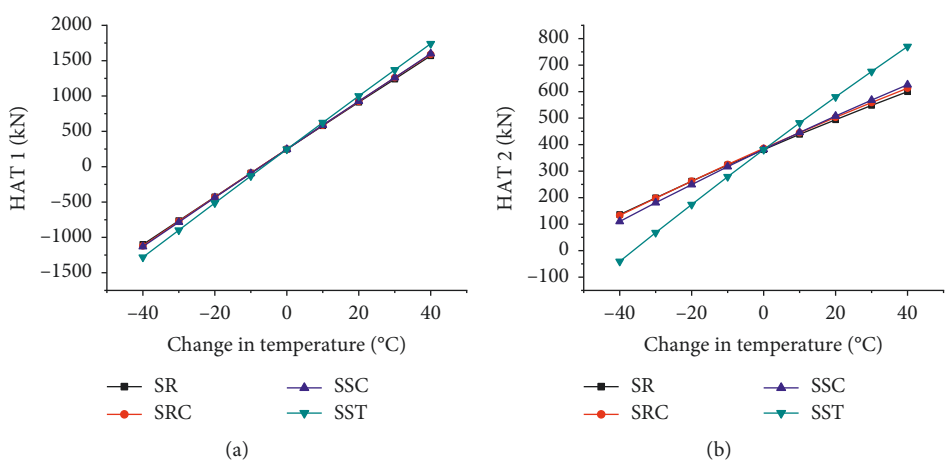

Figure 7: Relationship between the horizontal arch thrust and the temperature in the full-span load distribution. Change in (a) HAT 1 and (b) HAT 2 with varying temperature.

while the cable forces of the other three structures changed in a similar manner. Moreover, the cable force of the CSBV with semiparallel steel tendon cables exhibits a greater change than that of the CSBV with the other three cable types owing to the large elastic modulus and thermal expansion coefficient of the SST cables.

Figure 11 shows the influence of the temperature on the force of the vertical struts in the half-span load distribution;

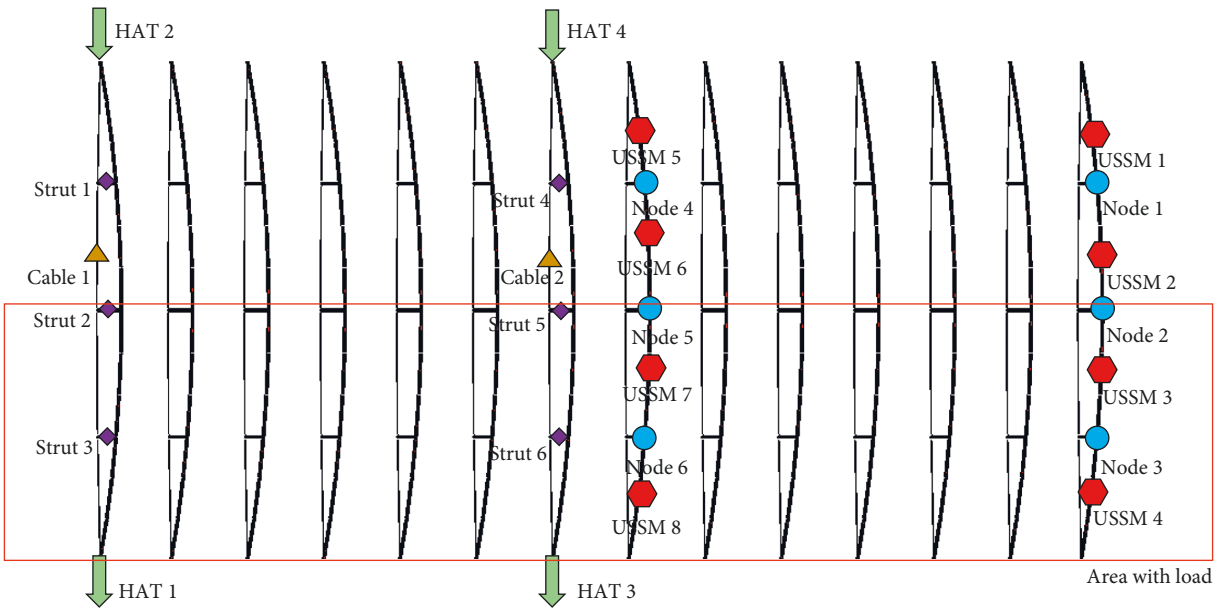

Figure 8: Targets in the numerical simulation analysis with a half-span load distribution.

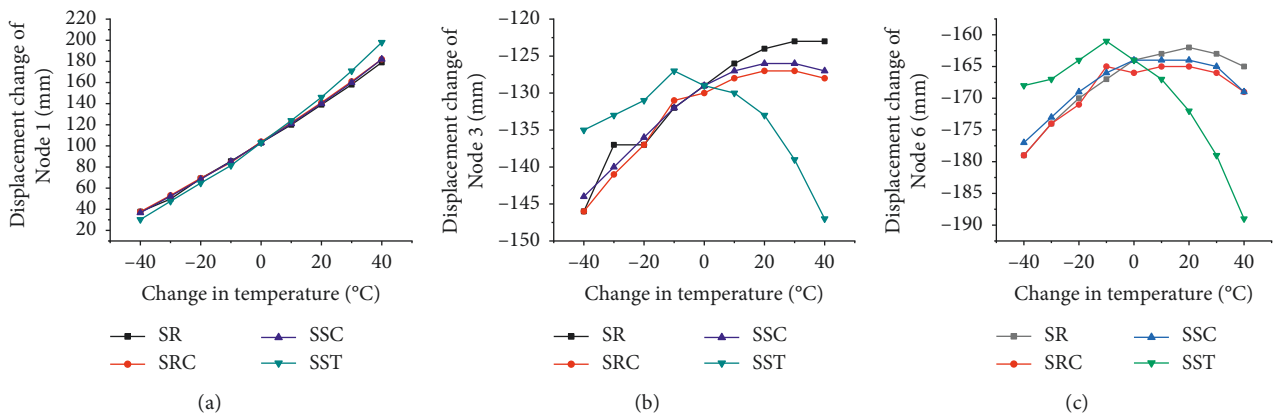

Figure 9: Relationship between the vertical displacement of nodes and the temperature in the half-span load distribution. Displacement of (a) Node 1, (b) Node 3, and (c) Node 6 with varying temperature.

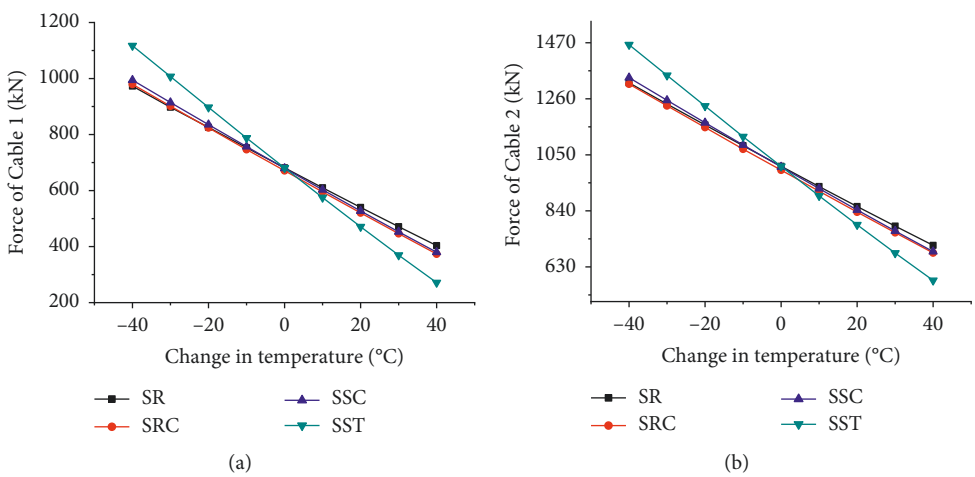

Figure 10: Relationship between the cable force at the end-frame and the temperature in the half-span load distribution. Change in the force of (a) Cable 1 and (b) Cable 2 with varying temperature.

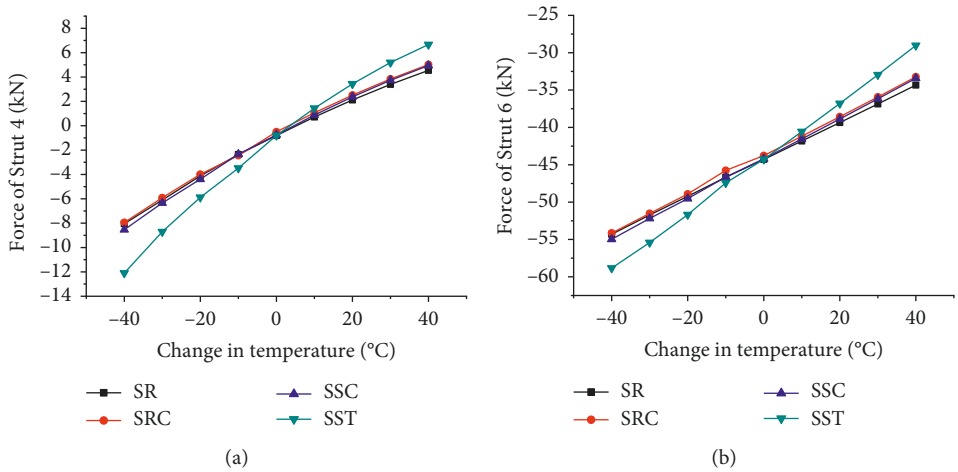

Figure 11: Relationship between the strut force and the temperature in the half-span load distribution. Change in the force of (a) Strut 4 and (b) Strut 4 with varying temperature.

the negative sign represents a pressure force. With increasing temperature, the strut pressure force decreases almost linearly. In the area without the load, the strut pressure force is less than that in the area with the load, as shown in Figure 11. Moreover, the strut pressure force of the CSBV with semiparallel cables exhibited a greater change than that of the CSBV with the other three cable types.

Figure 12 shows the relationship between the force of USSM and the temperature; the negative sign represents a pressure force, and the positive sign represents a tension force. Except for USSM 2, the relationship between the force of the USSM and the temperature is approximately linear. However, the change in the force of USSM 2 is smaller than that of the other members. The change in the force of USSM 4 with increasing temperature is similar to that of USSM 1; the force decreases linearly with increasing temperature, as shown in Figure 12(a). The change in the forces of USSM 5–8 is similar to that of USSM 3; the force increases with increasing temperature, as shown in Figure 12(c). Moreover, the effect of temperature on the force of the upper steel member in the CSBV with semiparallel cables is noticeably different than that of the other structures.

Figure 13 shows the relationship between the horizontal arch thrust and the temperature under the half-span load; the negative sign represents an opposite horizontal arch thrust, i.e.,the horizontal arch produces tension. The horizontal arch thrust increases linearly with increasing temperature. The change in the horizontal arch thrust is larger in the end-frame than in the midframe. Moreover, the change in the horizontal thrust for the CSBV with semiparallel steel tendon cables is more obvious than that in the other three structures.

2.4. Dynamic Characteristics of CSBV. Considering the effect of the prestress, the first 10 vibration modes were calculated using the block Lanczos method, and the results are given in Tables 2–5. The results indicate that with increasing temperature, the frequency of the CSBV decreases linearly. Moreover, the change in the frequency of the CSBV with semiparallel steel tendon cables is larger than that in the other structures.

2.5. Numerical Simulation of the Seismic Response of CSBV Structures. To investigate the effect of the temperature on the seismic response of the CSBV, a seismic wave is selected to perform a transient analysis on the structure. The roof load ($1.0 \times 0.8\,\mathrm{kN/m^2} + 0.5 \times 0.5\,\mathrm{kN/m^2}$) was applied to each node of the reticulated shell in the form of a concentrated mass. This transient analysis is performed using the Full method, which includes the Rayleigh damping:

$$[C] = \alpha[M] + \beta[K]. \tag{1}$$

In equation (1), α and β have the following relationships with the viscous proportional damping coefficient, ξ:

$$\alpha = \frac{4\pi f_1 f_2 \xi}{f_1 + f_2}, \tag{2}$$

$$\beta = \frac{\xi}{\pi f_1 + \pi f_2}. \tag{3}$$

In equations (2) and (3), ξ is 0.02 and f_1 and f_2 are the frequencies of the first and second vibration modes, respectively, which are given in Tables 2–5. After the time-history analysis, the maximum displacement of the nodes, cable force, strut force, USSM force, and reaction force can be obtained. The test cases are similar to the simulation of the half-span load distribution shown in Figure 8. The seismic responses are shown in Figure 14, including the displacement, cable force, and horizontal arch thrust. The displacement of the nodes (Figure 14(a)), the cable force (Figure 14(b)), and the horizontal arch thrust (Figure 14(d)) changed linearly with increasing temperature. The change in the strut force with increasing temperature is not linear, but as the maximum change in the strut force is only approximately 30 kN, it can be considered to be linear. The change in the USSM force (Figure 14(e)) with increasing temperature differs from the other parameters. For the USSM

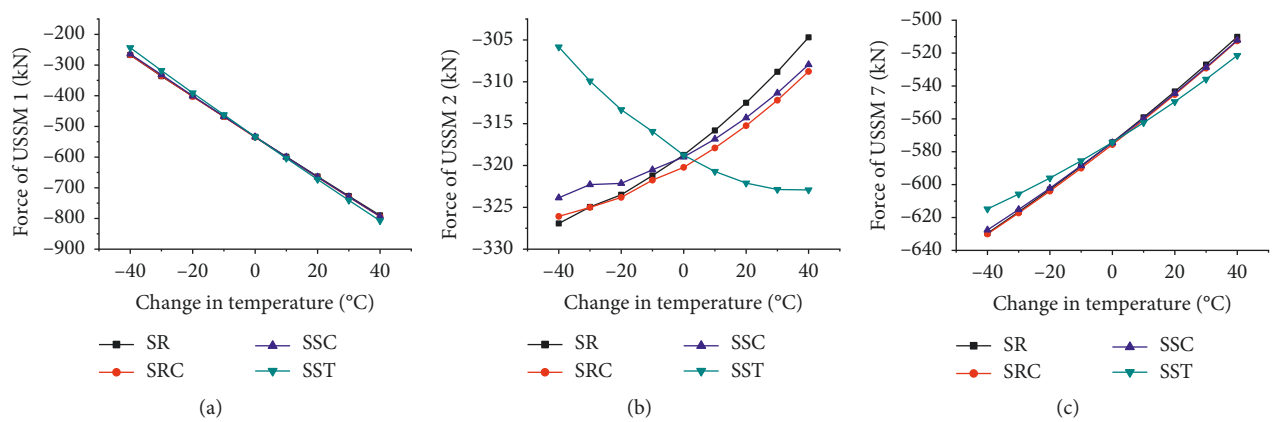

Figure 12: Relationship between the force of upper structural steel members and the temperature in the half-span load distribution. Change in the force of (a) USSM 1, (b) USSM 2, and (c) USSM 7 with varying temperature.

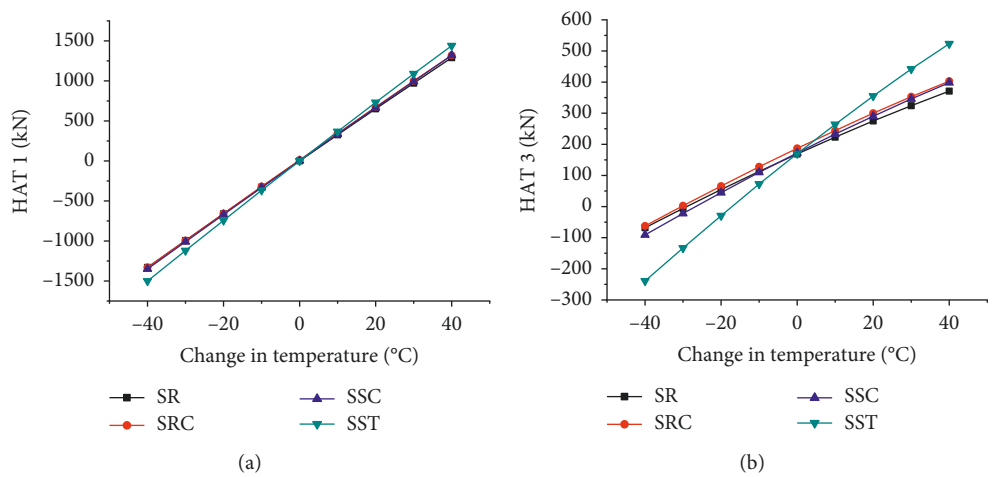

Figure 13: Relationship between the horizontal arch thrust and the temperature in the half-span load distribution. Change in (a) HAT 1 and (b) HAT 3 with varying temperature.

Table 2: Frequencies of the first 10 vibration modes of the CSBV with steel rod cables (unit: Hz).

Temperature (°C)	−40	−30	−20	−10	0	10	20	30	40
f_1	1.6304	1.6243	1.6181	1.612	1.6058	1.5996	1.5933	1.587	1.5807
f_2	1.8617	1.8533	1.8449	1.8364	1.8279	1.8193	1.8106	1.802	1.7932
f_3	2.3709	2.3596	2.3483	2.3368	2.3251	2.3134	2.3016	2.2896	2.2775
f_4	2.8177	2.8099	2.8020	2.7941	2.7861	2.7781	2.7700	2.7619	2.7537
f_5	2.8893	2.8807	2.8721	2.8633	2.8545	2.8456	2.8367	2.8277	2.8186
f_6	3.0043	2.9893	2.9740	2.9586	2.9429	2.9270	2.9110	2.8947	2.8782
f_7	3.0488	3.0377	3.0266	3.0153	3.0039	2.9924	2.9808	2.9691	2.9573
f_8	3.3223	3.3075	3.2925	3.2773	3.2619	3.2463	3.2305	3.2145	3.1983
f_9	3.6366	3.6168	3.5967	3.5762	3.5555	3.5344	3.5129	3.4912	3.4691
f_{10}	3.7133	3.694	3.6744	3.6545	3.6343	3.6138	3.5930	3.5719	3.5504

located in the side span, the USSM force changes linearly with increasing temperature. For the USSM located in the middle span, the force changes approximately linearly from −30°C to +40°C. Moreover, the change in the seismic responses of the CSBV having semiparallel steel tendons with temperature was larger than those in the other structures.

3. Experimental Verification

To verify the finite element model of the CSBV experimentally in a convenient manner, a scale model was designed. Corresponding numerical simulations and experiments were then performed.

Table 3: Frequency of the first 10 vibration modes of the CSBV with steel wire rope cables (unit: Hz).

Temperature (°C)	−40	−30	−20	−10	0	10	20	30	40
f_1	1.6296	1.6233	1.6171	1.6108	1.6045	1.5981	1.5918	1.5853	1.5789
f_2	1.8611	1.8526	1.8440	1.8354	1.8267	1.8180	1.8092	1.8004	1.7915
f_3	2.3706	2.3592	2.3477	2.3361	2.3244	2.3125	2.3006	2.2885	2.2763
f_4	2.8174	2.8095	2.8015	2.7934	2.7853	2.7771	2.7689	2.7606	2.7523
f_5	2.8891	2.8804	2.8715	2.8626	2.8537	2.8446	2.8355	2.8264	2.8171
f_6	3.0043	2.9891	2.9737	2.9582	2.9425	2.9265	2.9103	2.8940	2.8774
f_7	3.0487	3.0374	3.0261	3.0146	3.0031	2.9914	2.9797	2.9678	2.9558
f_8	3.3222	3.3073	3.2921	3.2768	3.2612	3.2455	3.2295	3.2133	3.1970
f_9	3.6367	3.6168	3.5966	3.5760	3.5552	3.5340	3.5125	3.4907	3.4685
f_{10}	3.7133	3.6939	3.6741	3.6541	3.6338	3.6131	3.5921	3.5708	3.5492

Table 4: Frequency of the first 10 vibration modes of the CSBV with steel strand cables (unit: Hz).

Temperature (°C)	−40	−30	−20	−10	0	10	20	30	40
f_1	1.6313	1.6250	1.6186	1.6121	1.6056	1.5991	1.5926	1.5860	1.5794
f_2	1.8626	1.8540	1.8453	1.8366	1.8278	1.8189	1.8100	1.8010	1.7920
f_3	2.3717	2.3602	2.3486	2.3369	2.3251	2.3131	2.3010	2.2888	2.2765
f_4	2.8190	2.8108	2.8026	2.7943	2.786	2.7777	2.7692	2.7608	2.7522
f_5	2.8906	2.8817	2.8727	2.8636	2.8544	2.8452	2.8359	2.8265	2.8171
f_6	3.0050	2.9898	2.9743	2.9587	2.9429	2.9268	2.9105	2.8941	2.8773
f_7	3.0501	3.0387	3.0272	3.0155	3.0038	2.9920	2.9800	2.9679	2.9557
f_8	3.3236	3.3084	3.2931	3.2776	3.2618	3.2459	3.2298	3.2135	3.1969
f_9	3.6373	3.6173	3.597	3.5764	3.5554	3.5342	3.5126	3.4906	3.4683
f_{10}	3.7145	3.6949	3.675	3.6548	3.6343	3.6135	3.5923	3.5709	3.5491

Table 5: Frequency of the first 10 vibration modes of the CSBV with semiparallel steel tendons (unit: Hz).

Temperature (°C)	−40	−30	−20	−10	0	10	20	30	40
f_1	1.6377	1.6298	1.6218	1.6138	1.6058	1.5977	1.5895	1.5813	1.5731
f_2	1.8686	1.8586	1.8484	1.8382	1.8279	1.8175	1.8071	1.7965	1.7860
f_3	2.3768	2.3640	2.3512	2.3382	2.3251	2.3119	2.2985	2.2850	2.2714
f_4	2.8266	2.8165	2.8065	2.7963	2.7861	2.7758	2.7655	2.7551	2.7446
f_5	2.8985	2.8876	2.8767	2.8656	2.8545	2.8433	2.8320	2.8206	2.8092
f_6	3.0093	2.9930	2.9765	2.9598	2.9429	2.9258	2.9084	2.8908	2.8730
f_7	3.0580	3.0446	3.0312	3.0176	3.0039	2.9901	2.9761	2.9620	2.9478
f_8	3.3310	3.3140	3.2969	3.2795	3.2619	3.2441	3.2261	3.2078	3.1893
f_9	3.6410	3.6201	3.5989	3.5773	3.5555	3.5332	3.5107	3.4878	3.4645
f_{10}	3.7212	3.7000	3.6784	3.6565	3.6343	3.6118	3.5889	3.5657	3.5421

3.1. Scale Model. To facilitate the experiments, a CSBV structure was designed. The span, length, rise, and sag of the prototype are 3.333 m, 3.587 m, 0.3 m, and 0.05 m, respectively. A total of seven cables are evenly spaced in the longitudinal direction, with three rods uniformly spaced in the span direction between each cable and the upper shell. The lower column height is 2.1 m.

Considering the market supply and the requirements of the welding, Q235B steel circular hollow sections with dimensions of 8 mm × 1 mm, 10 mm × 1 mm, and 12 mm × 1 mm are used. The upper barrel vault model is composed of three kinds of steel tube sections, including Φ8 mm × 1 mm, Φ10 mm × 1 mm, and Φ12 mm × 1 mm. The struts are steel tubes with sections of Φ12 mm × 1 mm. The columns are steel tube with sections of Φ50 mm × 2 mm and lengths of 2.1 m. The steel tubes are all Q235b, and the coefficient of thermal expansion is 1.20×10^{-5}/°C. High-strength steel wires with a diameter of 6 mm and tensile strength of 600 MPa are used as the cables.

3.2. Experimental Investigation. To verify the numerical results, an experimental investigation was carried out. According to the initial design, the experimental model is made of standard steel wire cables only. All of the bars in the upper barrel vault model are connected with welded hollow pipe joints. The ends of the upper barrel vault model are connected to the top of the column by welding. The tops of the struts are connected to the upper barrel vault model with one-way hinge bolt joints. The cable groove was used as a connection at the bottom end of the struts, while bolts were used to link the end of the cable with the top of column. By twisting these bolts, the cable forces could be adjusted to reach the design value. The cables were then fixed with cable

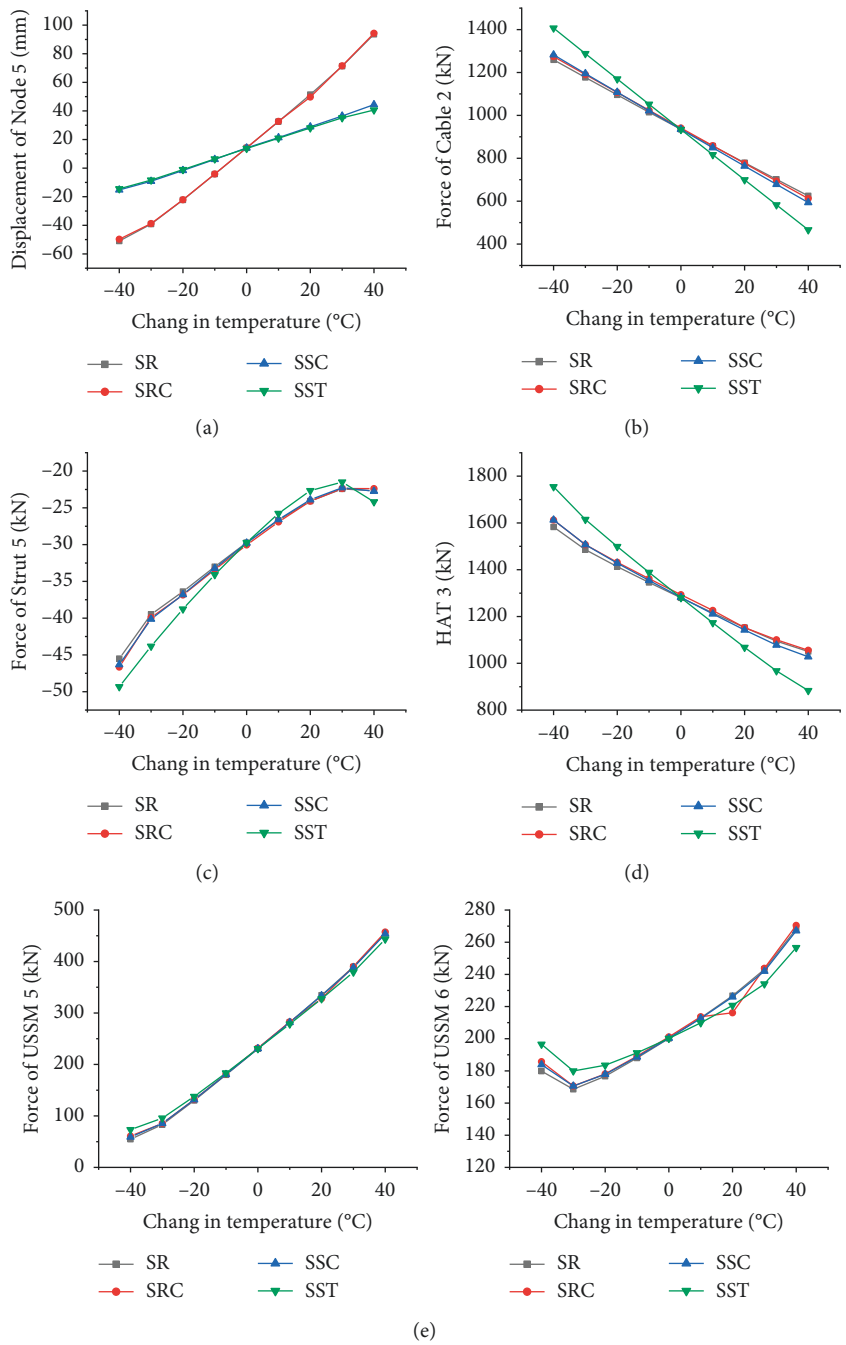

Figure 14: Changes in the maximum seismic response with varying temperature. (a) Change in the displacement of Node 5 with varying temperature. (b) Change in the cable force with varying temperature. (c) Change in the strut force with varying temperature. (d) Change in the horizontal arch thrust with varying temperature. (e) Change in the USSM force with varying temperature.

buttons to avoid slipping of the cables. The test model is shown in Figure 15(a).

The objective of these experiments is to measure the vertical displacement and stress of the vertical struts in the full-span load distribution and half-span load distribution. The loads were added using hanging sandbags (Figure 15(b)). To maintain consistency with the numerical analyses, 30 loading points were set in the full-span distribution, as shown in Figure 16(a), and 15 loading points were set in the half-span distribution, as shown in Figure 16(b).

During the experiments, the model was covered in a heat-retaining tent, as shown in Figure 15(c), and the lowest outdoor temperature was −7°C. The temperature inside the tent was measured with a thermometer, and the layout of the sensors is shown in Figure 16(c). According to preliminary measurements, the temperature inside the tent was steady at approximately −5°C. Electric stoves were used to heat the inside of the tent to a final temperature of 35°C. The layout of the displacement measuring points is shown in Figure 16(c) (D1–D3). The layout of the USSM strain measuring points is

(a) (b) (c)

Figure 15: Experimental model of the CSBV structure. (a) CSBV test model. (b) Sandbags hanging on the test model. (c) Heat-retaining tent outside the CSBV model.

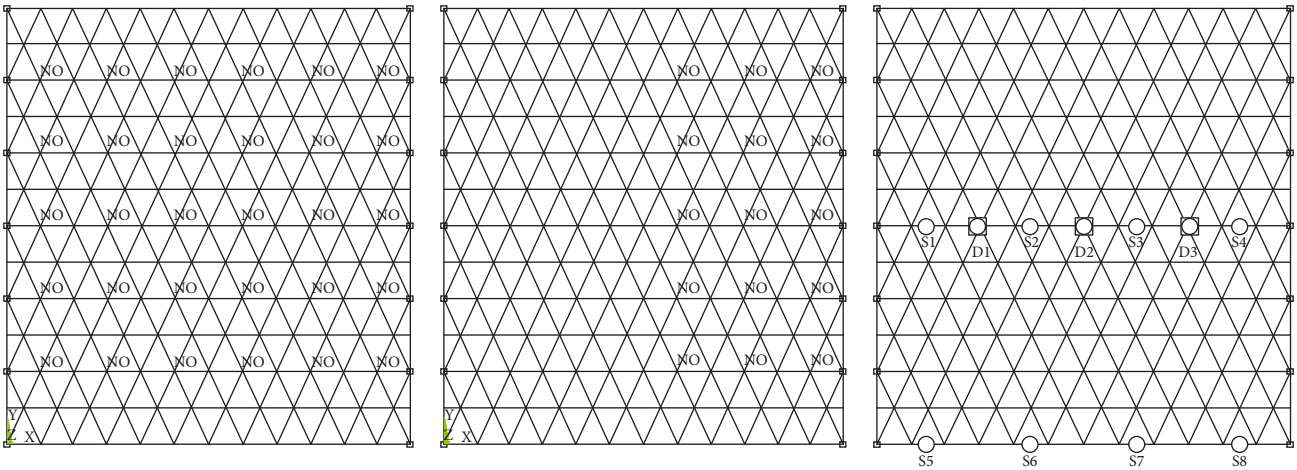

(a) (b) (c)

Figure 16: Layout of the sensors and loads on the CSBV. (a) Distribution of the hanging sandbags in the full span. (b) Distribution of the hanging sandbags in the half span. (c) Layout of the sensors on the CSBV.

also shown in Figure 16(c) (S1–S8). The USSM strains are measured with YE2539 high-speed static strain indicators, and a computer is employed as the strain measurement system. The structural displacements are measured with dial indicators.

The procedure for the experiments is as follows:

(1) Prepare the relevant experimental equipment: set up the electric stoves, thermometers, and dial indicators in the designated locations; debug the high-speed static strain indicator; and close the tent tightly to prevent heat dissipation

(2) Hang sandbags to load the full span according to Figure 16(a) and turn on the electric stoves to increase the temperature inside the tent from the initial −5°C; when the temperature in the tent reaches a stable 35°C, measure the displacements and stresses

(3) Turn off the electric stoves and open the tent to allow the model to return to the initial temperature (−5°C)

(4) Hang sandbags to load the half span according to Figure 16(b) and turn on the electric stoves to increase the temperature inside the tent from the initial −5°C; when the temperature in the tent reaches a stable 35°C, measure the displacements and stresses.

The actual project and scale model have different rise-span ratios and proportions of the component size and model size. Therefore, their internal force changes and displacements will differ. This experiment is only intended to demonstrate the validity of the finite element model of the CSBV.

As shown in Figures 17 and 18, as the temperature increases, the trends in the experimental and simulated vertical displacements are similar, although the displacement values differ greatly. Further, the displacement change measured in the experiments is not linear. However, because the temperature in the experiments could not be stabilized at specific values between −5 and 35°C, the value of the vertical displacement generated under temperatures other than 40°C will have some error. Therefore, the change in the vertical displacement in the experiments can be considered to be linear.

Figures 19 and 20 show comparisons of the change in the USSM stress in the experiments and finite element numerical simulations. Some error is introduced as a result of

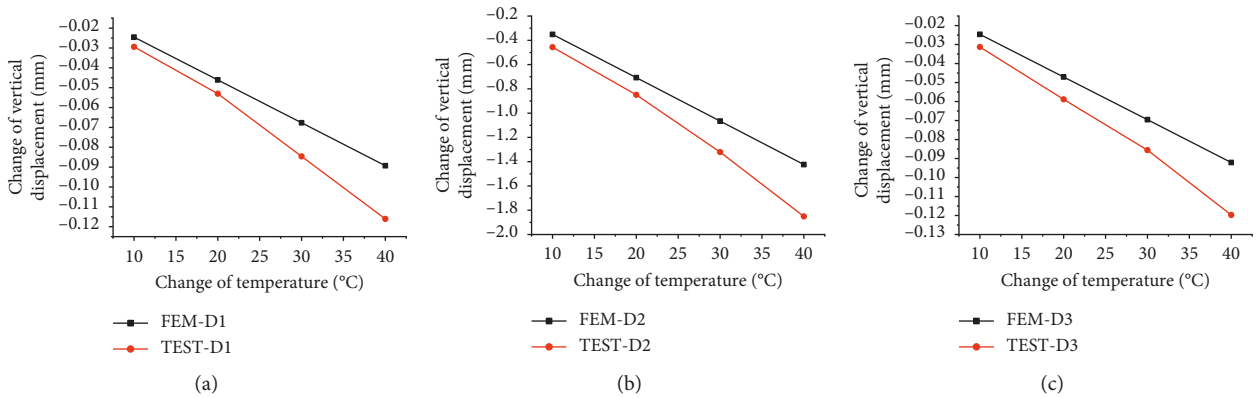

Figure 17: Comparison of the change in nodal displacement in the experiments and finite element numerical simulation under the full-span load. Displacement change of (a) D1, (b) D2, and (c) D3 under the full-span load.

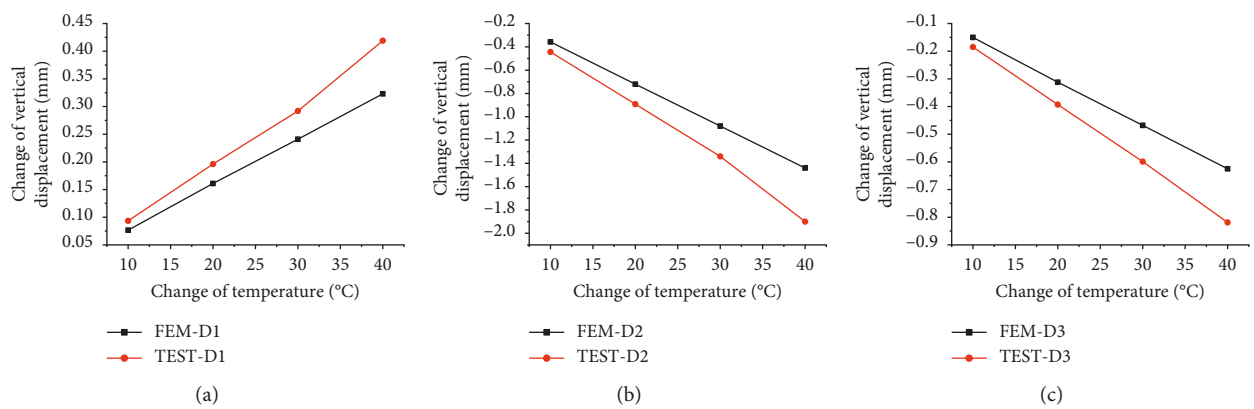

Figure 18: Comparison of the change in nodal displacement in the experiments and finite element numerical simulation under the half-span load. Displacement change of (a) D1, (b) D2, and (c) D3 under the half-span load.

flaws in the test model, boundary conditions, the temperature field, the precision of the measurements, etc. Except for the temperature field, these error sources are difficult to improve in the tests or numerical analysis. Owing to these errors, the values in the experiments were larger than those obtained with the finite element model. However, they have the same trends, and the change in the experimental values was approximately linear. Therefore, the finite element model of the CSBV is considered to be effective under varying temperature.

4. Conclusions

CSBV structures based on beam string structures (or truss string structures) and cylindrical lattice shells are a new type of hybrid spatial steel structures. The design of the cable-supported structure is different from that of other steel structures. In this study, a finite element model of a CSBV was built with the cable force determined through iterative calculation. A numerical investigation was carried out to obtain the temperature response of the CSBV. An experimental investigation with a physical model of the CSBV was then conducted under full-span loading and half-span loading. The following conclusions have been drawn:

(1) The changes in the vertical displacement and USSM stress in the experiment are a little larger than those in the finite element model, but the trends are the same. Further, considering the inevitable error, the experiment verified that the finite element model of the CSBV is effective under varying temperature.

(2) Under the full-span loading, the changes in the structure internal force and displacement can be considered linear in the CSBV design process. The cable force and strut force decrease with increasing temperature. Meanwhile, the horizontal arch thrust increases with increasing temperature. Moreover, the internal force of the CSBV with semiparallel cables exhibited a larger change than that of the CSBV with the other three cables.

(3) Under the half-span loading, the changes in the structure internal force and displacement can be considered linear in the CSBV design process. The cable force and strut force decrease with increasing

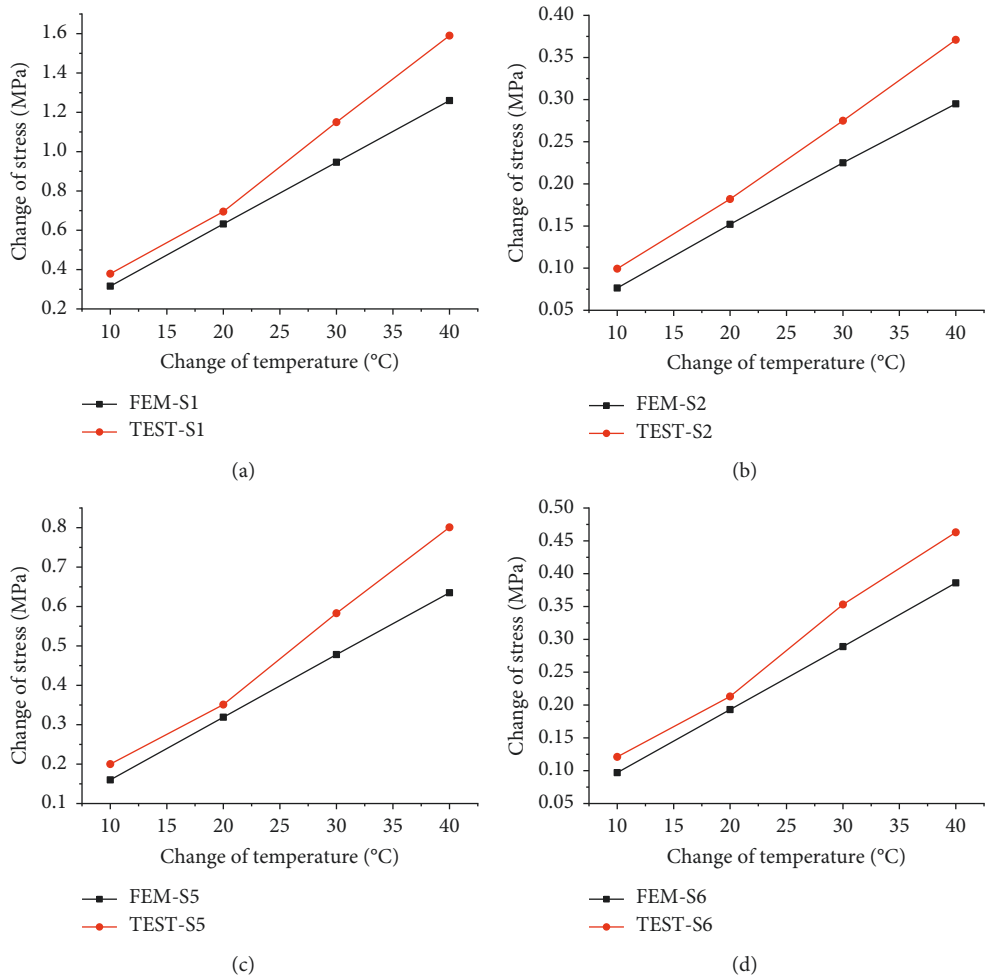

Figure 19: Comparison of the change in the USSM stress in the experiments and finite element numerical simulations under the full-span load. Change in the force of (a) S1, (b) S2, (c) S3, and (d) S6 under the full-span load.

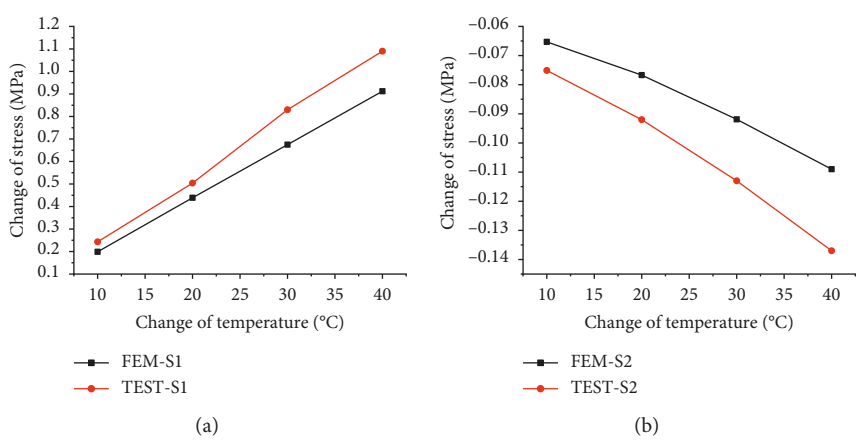

Figure 20: Continued.

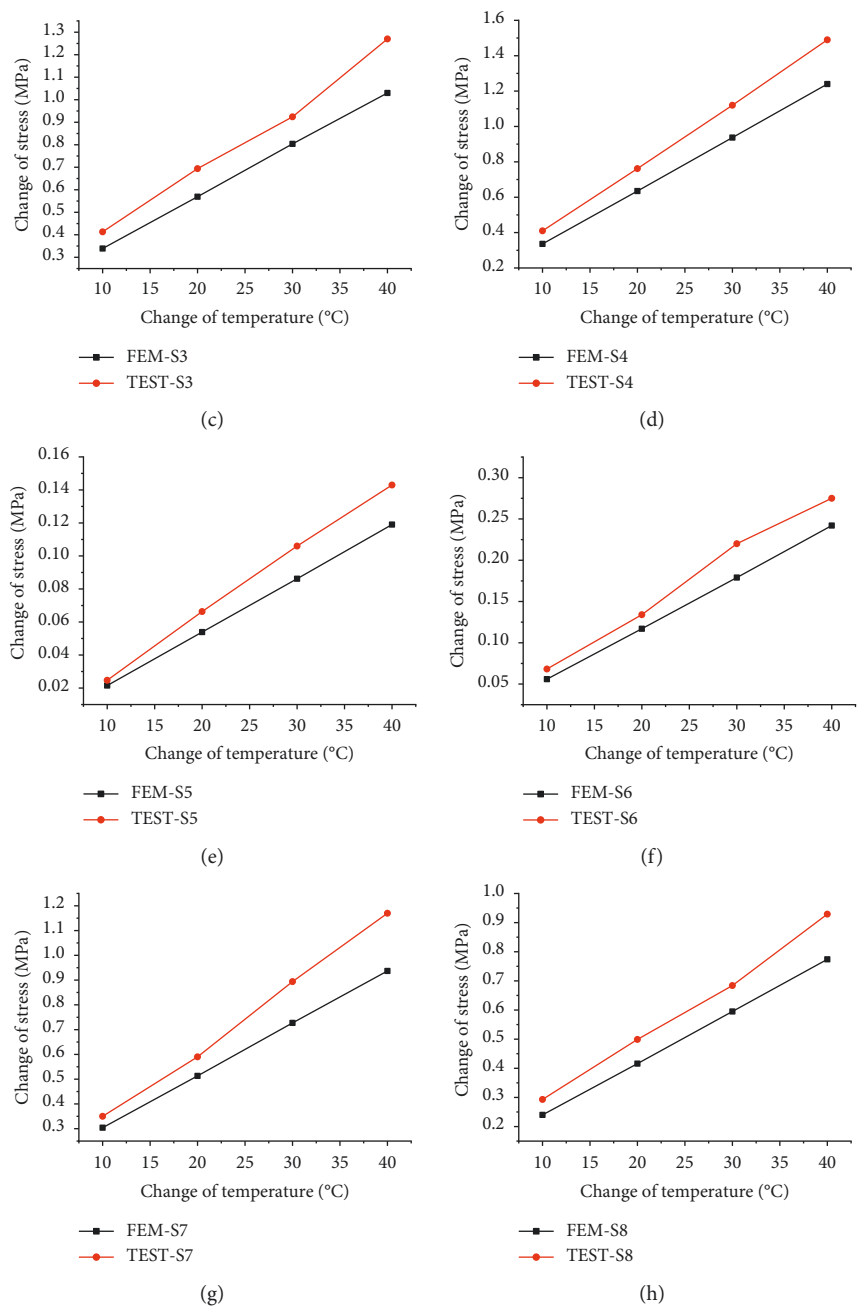

Figure 20: Comparison of the change in the USSM stress in the experiments and finite element numerical simulations under the half-span load. Change in the force of (a) S1, (b) S2, (c) S3, (d) S4, (e) S5, (f) S6, (g) S7, and (h) S8 under the half-span load.

temperature. Meanwhile, the horizontal arch thrust increases with increasing temperature. Moreover, the internal force of the CSBV with semiparallel cables exhibited a larger change than that of the CSBV with the other three cables.

(4) The frequency of the CSBV decreases linearly with increasing temperature. With the seismic response, the displacement, cable force, and horizontal arch thrust of structure change linearly with increasing temperature. The cable force decreases with increasing temperature, and the horizontal arch thrust decreases with increasing temperature.

(5) The internal force of the CSBV with semiparallel tendon cables is more sensitive to changes in the

temperature. Therefore, in area with large temperature changes, the semiparallel cables are not recommended as components in the CSBV design process, as these can increase the loss of the cable prestress with changes in temperature. Because cables with a high elastic modulus are beneficial for the static performance of the CSBV and steel wire rope cables have a low elastic modulus, steel rod and steel strand cables are recommended as components for CSBVs considering the effect of temperature.

Data Availability

The data used to support the findings of this study are included within the article.

Conflicts of Interest

The authors declare that there are no conflicts of interest regarding the publishing of this paper.

Acknowledgments

This work was sponsored by the National Nature Science Foundation of China (grant number 51408016), Natural Science Foundation of Tianjin (grant number 16JCQNJC07100), and the Scientific Research Program of Beijing Education Committee (grant number KM201710005017).

References

[1] Z. H. Chen, X. Y. Yan, W. T. Qiao et al., "Structure system of cable supported barrel vault structure," ZL200810053722.8, 2008, In Chinese.

[2] W. Qiao, Z. H. Chen, and M. S. Zhao, "Test study on basic static characteristics of cable supported barrel vault structure," *International Journal of Advanced Steel Structures*, vol. 8, no. 2, pp. 199–211, 2012.

[3] G. J. Sun, Z. H. Chen, and R. W. Longman, "Numerical and experimental investigation of the dynamic characteristics of cable supported barrel vault structure," *Journal of Mechanics of Materials and Structures*, vol. 8, no. 2, pp. 1–14, 2013.

[4] H. Liu, W. Zhang, H. Yuan, J. Zhu, and J. Zheng, "Modified double-controlform-finding analysis for suspendomes considering the construction process and the friction of cable-strut joints," *Engineering Structures*, vol. 120, pp. 75–81, 2016.

[5] F. Uzun, "Form-finding and analysis of an alternative tensegrity dome configuration," *Advances in Structural Engineering*, vol. 20, no. 11, pp. 1644–1657, 2017.

[6] J. Lu, X. Dong, X. Zhao, X. Wu, and G. Shu, "Form-finding analysis for a new type of cable-strut tensile structures generated by semi-regular tensegrity," *Advances in Structural Engineering*, vol. 20, no. 5, pp. 772–783, 2017.

[7] X. Liu, A. Zhang, X. Zhang, and C. Tian, "Particle swarm optimization algorithm for suspendome structure under multiple loading cases," *Engineering Computations*, vol. 33, no. 3, pp. 767–788, 2016.

[8] L.-M. Chen and S.-L. Dong, "Optimal prestress design and construction technique of cable-strut tension structures with multi-overall selfstress modes," *Advances in Structural Engineering*, vol. 16, no. 10, pp. 1633–1644, 2013.

[9] K. Li and D. Huang, "Static behavior of kiewitt6 suspendome," *Structural Engineering and Mechanics*, vol. 37, no. 3, pp. 309–320, 2011.

[10] Q.-S. Cao and Z.-H. Zhang, "A simplified strategy for force finding analysis of suspendomes," *Engineering Structures*, vol. 32, no. 1, pp. 306–318, 2010.

[11] Z. Chen, R. Z. Yan, and X. D. Wang, "Experimental researches of a suspen-dome structure with rolling cable-strut joints," *Advanced Steel Construction*, vol. 1, no. 11, pp. 15–38, 2015.

[12] H. J. Liu, L. F. Yang, and Y. F. Luo, "Dynamic stability of large-spansuspen-domessubjected to seismic excitations," *Advanced Materials Research*, vol. 378-379, pp. 209–212, 2012.

[13] Z. Chen, W. Qiao, and X. Yan, "Cable supported barrel vault structure system and research on mechanics feature," *Advanced Steel Construction*, vol. 6, no. 3, pp. 867–878, 2010.

[14] J. Cai, Y. Q. Liu, and F. Jian, "Nonlinear stability analysis of a radially retractable suspen-dome," *Advanced Steel Construction*, vol. 13, no. 2, pp. 117–131, 2017.

[15] L.-M. Chen, H. Deng, Y.-H. Cui, S.-L. Dong, and Y.-Y. Zhou, "Theoretical analysis and experimental study on sensitivity of element-length error in cable-strut tensile structures," *Advances in Structural Engineering*, vol. 19, no. 9, pp. 1463–1471, 2016.

[16] P. Li, M. Wu, and P. Xing, "Novel cable-stiffenedsingle-layer latticed shells and their stabilities," *Journal of Constructional Steel Research*, vol. 92, pp. 114–121, 2014.

[17] J. Guo, "Research on distribution and magnitude of initial geometrical imperfection affecting stability of suspen-dome," *Advanced Steel Construction*, vol. 7, pp. 344–358, 2011.

[18] P. Li, M. Wu, H. Wang, and M. Shi, "Experimental and numerical analysis of cable-stiffenedsingle-layer spherical latticed shells," *Advances in Structural Engineering*, vol. 19, no. 3, pp. 488–499, 2016.

[19] Z. Chen, Z. Liu, and G. Sun, "Thermal behavior of steel cables in prestressed steel structures," *Journal of Materials in Civil Engineering*, vol. 23, no. 9, pp. 1265–1271, 2011.

[20] G. Sun, Z. Chen, and Z. Liu, "Analytical and experimental investigation of thermal expansion mechanism of steel cables," *Journal of Materials in Civil Engineering*, vol. 23, no. 7, pp. 1017–1027, 2011.